

NANO EXPRESS

Open Access

Multi-channel Si-liquid crystal filter with fine tuning capability of individual channels for compensation of fabrication tolerances

Anna Baldycheva^{1*}, Vladimir A Tolmachev², Kevin Berwick³ and Tatiana S Perova^{1*}

Abstract

In this study, a technique for the optimization of the optical characteristics of multi-channel filters after fabrication is proposed. The multi-channel filter under consideration is based on a Si photonic crystal (PhC), tunable liquid crystal and opto-fluidic technologies. By filling air grooves in the one-dimensional, Si-Air PhC with a nematic liquid crystal, an efficiently coupled multi-channel filter can be realised in which a wide stop band is used for channel separation over a wide frequency range. By selectively tuning the refractive index in various coupled cavities, continuous individual tuning of the central channel (or edge channels) up to 25% of the total channel spacing is demonstrated. To our knowledge, this is the first report on the electro-optical solution for the compensation of fabrication tolerances in an integrated platform.

Keywords: Multi-cavity photonic crystal, Coupled Fabry-Pérot resonators, Liquid crystal devices, Integrated optics devices, Wavelength filtering devices, Lithography error, Line-width variation, Critical dimension variation

PACS: 42.60.Da, Resonators, Cavities, Amplifiers, Arrays, Rings, 42.60.Fc, Modulation, Tuning, Mode locking, 42.70.Df, Liquid crystals

Background

Although Si fabrication technology has significantly developed over the last 20 years, one of the main problems for optical, nano-scale periodic structures, such as Fabry-Perot interferometers and multi-channel photonic crystal (PhC) filters, remains in defining of the critical dimensions precisely in the system [1-3]. In general, structural deviations and non-uniformities present in the patterned features on the wafer occur for three principal reasons. First of all, there is the fundamental diffraction limit of the projection optics. Secondly, the mask pattern differs from the original design due to limitations in the mask fabrication process. Finally, random and systematic variations inevitably occur in a multitude of lithographic process parameters, such as focus and exposure [4]. Fabrication tolerances for modern e-beam lithography are usually assumed to be a minimum of about 5% to 10% of the nominal target dimensions. This crucially affects the optical characteristics of multi-channel filter devices

[5-7]. It changes the precise wavelength position of individual channels; it increases the out-of-band reflection and causes an attenuation of the maximum intensity, resulting in a lowering of the quality factor, Q . One of the most promising solutions to these problems may be a filter device with low-power and low-loss capability to compensate for the optical filter deviations. This would allow fine tuning of individual channels in the filter system by varying the temperature or by applying an electric field. However, one of the main challenges in the realisation of tunable multi-channel devices remains the fixed channel spacing or free spectral range which cannot be easily tuned due to the strong coupling between channels. One of the more successful attempts to tackle this problem was presented in [8], where the authors demonstrated a solution for an integrated platform. This approach requires the incorporation of metallic micro-heaters into large 245 μm resonators, demanding precise temperature control of the device during operation.

To our knowledge, there have been no reports in the literature on addressing this problem using electro-tuning for the individual channels in a multi-channel

* Correspondence: baldycha@tcd.ie; perovat@tcd.ie

¹Department of Electronic and Electrical Engineering, Trinity College Dublin, College Green, Dublin 2, Ireland

Full list of author information is available at the end of the article

system that is compatible with complementary metal oxide semiconductor technology. The design of the tunable multi-channel filter proposed in this work is based on a one-dimensional (1D) Si photonic crystal (PhC) using opto-fluidics and liquid crystal (LC) technologies [2,5,9-14]. An LC is one of the most attractive tuning material for Si-based integrated devices, enabling tuning of the resonance modes using low applied voltages (from 1.5 V) with negligible absorption during device operation. By creating optical cavities within the periodic structure by infiltration with LC, the PhC mirror can be transformed into a highly efficient coupled multi-channel filter [15]. A coupled multi-cavity PhC system has significant advantages over other types of coupled resonators in terms of device simplicity, ease of integration on a Si chip, and power consumption. We extended the continuous fine-tuning capability of LC single microcavity to a system of individually tunable coupled multi-cavities. The application of an electric field to each cavity was done individually, and its continuous selective variation across all cavities allows to overcome the problems related to the strong coupling between channels. Using an example of a coupled triple-cavity PhC filter operated using the first SBs, we have developed a simple model for easier manipulation of the LC within individual cavities, enabling the independent fine tuning of each channel in the overall system. We note that the model suggested can be extended to a higher number of coupled cavities (defects) and, therefore, to a higher number of resonances, with an improved Q value.

Methods

A free-spaced, microstructured, grooved Si structure, with quarter-wavelength Si-Air layers of optical thicknesses $n_{\text{Si}}d_{\text{Si}} = n_{\text{air}}d_{\text{air}} = m\lambda_m/4$ (where m is the order of the stop bands, SBs), is considered here as a model for an ordinary 1D PhC mirror. The refractive index of air, n_{air} , is 1, while the refractive index of Si is taken as $n_{\text{Si}} = 3.48$. The coupled resonators-induced transparency around the wavelength λ_m occurs when optical or geometrical defects are introduced into the perfect periodic structure (Figure 1) [16,17].

The creation of a microcavity resonator requires a doubling of the optical thickness of certain grooves, $n_{\text{def}}^{(i)}d_{\text{air}} = m\lambda_m/2$, where i is the number of the groove. This can be achieved, for example, by infiltration of the groove with filler with a suitable refractive index. By varying the optical thicknesses of the defects simultaneously, the resonance (or channel) peak positions, λ_c , and the Q factor of the coupled resonances obtained can be continuously tuned within the stop band (SB) [5,18,19]. For this purpose, the LC is a promising candidate material, with its capability of continuous reverse

tuning of the refractive index over a wide range of values by the application of a voltage, V [20]. In this study, we use the commercially available nematic LC E7 available by Merck KGaA, Darmstadt, Germany, which demonstrates a high anisotropy of the refractive index ($\Delta n = 1.7472 \dots 1.5217$) under applied voltages, $V = 1.5 \dots 15$ V [11-14]. For clarity, we consider an initial switching position that can achieve the same intermediate orientation of the LC molecules in all cavities. That is, it produces the average refractive index $n_{\text{LC}} = (1.7472 + 1.5217)/2 = 1.63$ at a switching voltage of approximately 10 V.

All modelled results are obtained using numerical simulations based on a transfer matrix method (TMM) [21]. The optimal design parameters for the LC-coupled microcavities, d_{Si} , d_{air} and $d_{\text{def}} = d_{\text{LC}}$, which give the highest Q factor and the narrowest equal wavelength spacings between the channels, λ_s , are determined using a graphical engineering approach, based on a Gap Map (GM) presentation [22]. The methodology of this approach is quite general and is described in detail in references [5,15,20]. In brief, optimal design parameters are determined by certain range of filling fractions, $\Delta f_{\text{Si}} = d_{\text{Si}}/a$, that correspond to the central part of the resonance lines within the SB on the GM and demonstrate the same improved optical characteristics, λ_s and Q . Depending on the order of the SB and the resonances within it, this Δf_{Si} range varies. For example, for the triple-channel PhC device considered here (Figure 1), the filling fractions ranges are $\Delta f_{\text{Si}} = 0.15 \dots 0.25$ (for the first order SBs), $\Delta f_{\text{Si}} = 0.35 \dots 0.45$ (for the second order SBs) and $\Delta f_{\text{Si}} = 0.47 \dots 0.57$ (for the third order SBs). Table 1 gives the TMM-simulated optimal design parameters, together with the optical characteristics of the sample triple-channel device [5].

Results and discussion

Optimal parameters taken from Table 1 were used for the fabrication of integrated triple-channel devices on a $\langle 100 \rangle$ p -type silicon-on-insulator (SOI) wafer with a device layer thickness of 4.5 μm . The fabrication process involved used e-beam lithography to define the patterns followed by plasma etching down to the buried oxide layer. Scanning electron microscopy (SEM) investigation of the devices fabricated revealed the presence of a random deviation of the Si wall thicknesses, δd_{Si} , of up to 10.8% of the target thickness. In Figure 2a, this deviation is demonstrated on the SEM image of the structure with $a = 900$ nm, which operates within the second order SB ($m = 2$, Table 1). This thickness deviation, δd_{Si} , directly influences the optical thicknesses of the cavities, $n_{\text{def}}^{(i)}d_{\text{air}} = n_{\text{def}}^{(i)}(a - d_{\text{Si}} \pm \delta d_{\text{Si}})$, and also the optical thicknesses of the spacings between the cavities (or optical

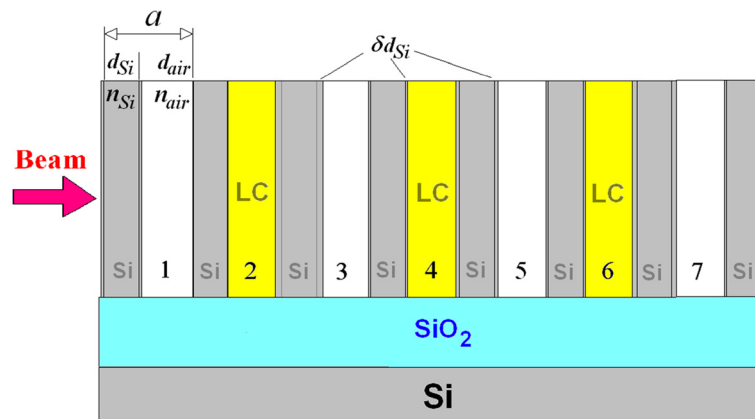


Figure 1 Schematic diagram of a 7.5 period, 1D, PhC with triple LC defects. The defects are realised in the second, fourth, and sixth periods (denoted by numbers). A Si wall thickness with fluctuation $\pm \delta d_{Si}$ in each lattice period causes a variation of groove thickness $d_{air} = a - d_{Si} \pm \delta d_{Si}$. The lattice constant is $a = d_{Si} + d_{air}$. The optical contrast of the defect-free PhC is n_{Si}/n_{air} .

thickness of the air grooves), $n_{air} d_{air} = n_{air} (d_{air} \pm \delta d_{Si})$. Variation of the geometrical parameters of a coupled-cavity device results in random shifts, splitting and attenuation of each of the cavity resonances [14;23-25].

Simulated transmission spectra for the devices originally designed and fabricated are demonstrated in Figure 2b,c,d. Although the attenuation of the maximum transmission intensities is only about 3% to 5% resulting in a negligible reduction in the parameter Q , the precise wavelength position of each channel, λ_c , was affected significantly. All of the channels are unequally blue/red-shifted by approximately 0.3% to 1.2% from the originally designed operational wavelengths, which is more than the target channel bandwidth (Figure 2b,c,d, red lines). A summary of the TMM analysis for the three fabricated structures, operating within the first three SBs along with data on the SEM registered thickness deviations, $\pm \delta d_{Si}$, and the corresponding random shifts of the resonant peak wavelengths, $\pm \Delta \lambda_{c1,2,3}$, are reported in Table 2.

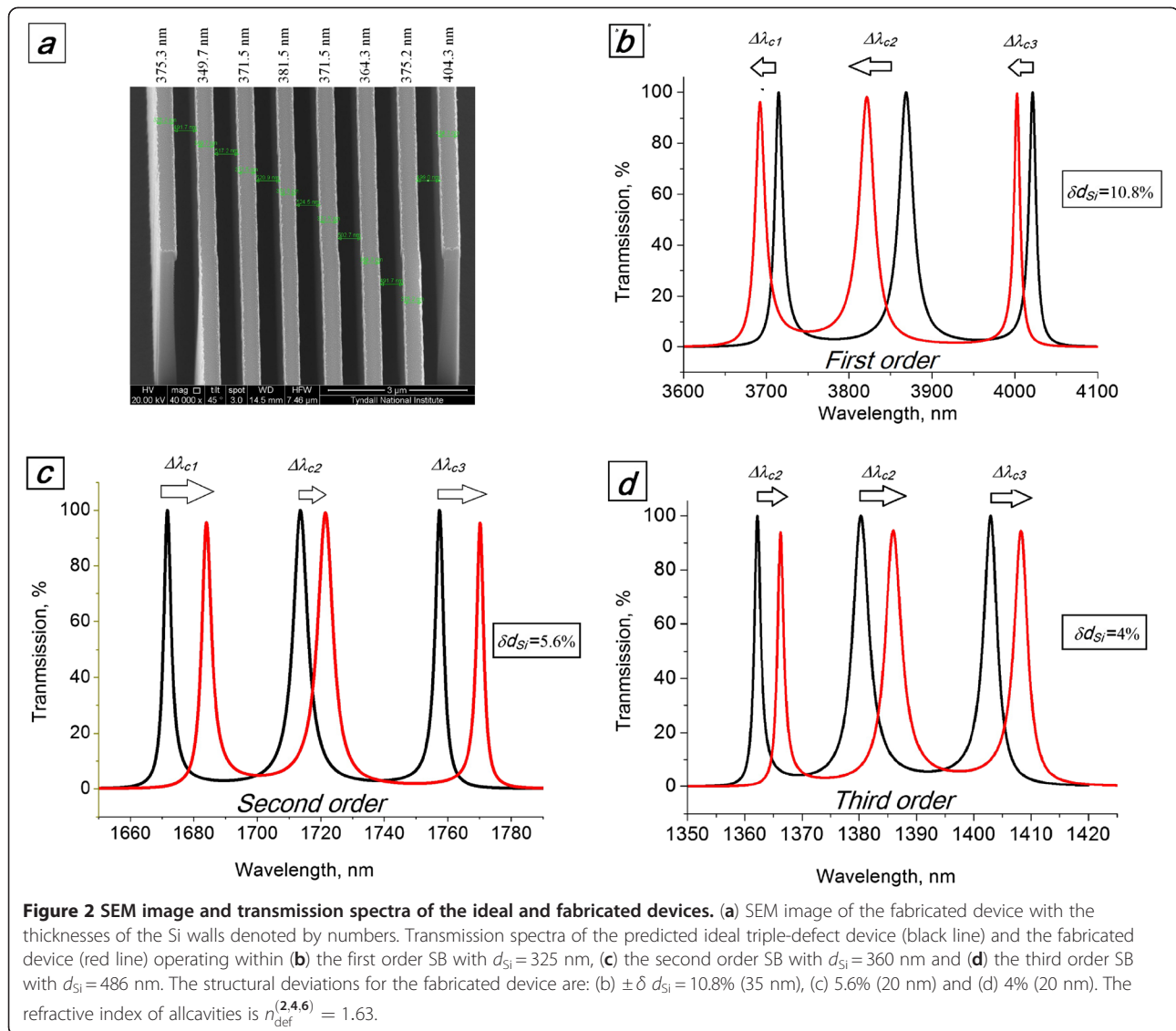
The simplest way to compensate for these errors, post-fabrication ($d_{air} \pm \delta d_{Si}$), is to adjust the refractive indices of the coupled cavities individually to their optimised values, $n_{def}^{(2,4,6)} \pm \delta n_{def}^{(2,4,6)}$. This can be achieved by fabrication of the device on SOI platform and by applying a different voltage to each individual cavity. Then, by increasing or decreasing the applied voltage by ΔV in the various cavities, different variations in the LC refractive indices can be obtained, $n_{def}^{(2,4,6)} = n_{LC} \pm \Delta n$. For the example of a triple-cavity PhC, we focus on the two most

obvious relationships between $n_{def}^{(2)}$, $n_{def}^{(4)}$ and $n_{def}^{(6)}$, allowing precise manipulation of the central channel position, λ_{c2} , or the edge-channel positions, λ_{c1} and λ_{c3} .

Let us gradually increase the refractive index of the central cavity, $n_{def}^{(4)} = n_{LC} + \Delta n$, by $\Delta n = 0.001$, while decreasing the refractive indices of the two edge cavities, $n_{def}^{(2)} = n_{def}^{(6)} = n_{LC} + \Delta n$ by the same value of Δn (Figure 3a). In this case, the central cavity has the strongest coupling, $n_{def}^{(2,6)} = n_{def}^{(2,6)} + 2\Delta n$, and acts as the primary cavity in the system, while the edge cavities represent variable mirrors on both sides of the central cavity. At the same time, the overall optical thickness of the system $n_{def}^{(2,4,6)} d_{air} = \lambda_m/2$ decreases which leads to a blue shift of its resonance peaks [15]. Let us monitor the positions of the triple resonances during these refractive index variations. We use normalised wavelength units, $NW = \lambda/a$, and therefore, the results obtained can be applied to a variety of nano- and micro- structures, operating over a wide wavelength range. In Figure 3b, we demonstrate transmission spectra for $\Delta n = 0.013$ (thin blue line) and $\Delta n = 0.026$ (thick blue line). The central channel is blue-shifted, while the edge resonances have retained their positions. For the example considered, the maximum refractive index difference, $2\Delta n = 0.052$ (which is only 24% of the birefringence value for the LC E7, $\Delta n_{E7} = 0.2255$), allows us to achieve a maximum relative independent shift of the central channel, $\Delta \lambda_s$, of up to 25% of the channel spacing, λ_s . However, further

Table 1 Optimal design parameters and channel characteristics of the first, second, third order SBs of triple-cavity PhC

m	$a = d_{Si} + d_{air}$ (nm)	f_{Si}	d_{Si} (nm)	λ_{c1} (nm)	λ_{c2} (nm)	λ_{c3} (nm)	$\lambda_s = \lambda_{s12} = \lambda_{s23}$ (nm)	Q	$I_{1,2,3}$ (%)
1	1,400	0.23	325	3,720	3,875	4,025	153.3	130	100
2	900	0.4	360	1,670	1,713	1,756	43	380	100
3	900	0.54	486	1,363	1,383	1,403	20	460	100



increases in the overall difference, $2\Delta n$, will break the symmetry of the system and initiate a coupling effect between all of the cavities, resulting in a shift of all the resonances simultaneously.

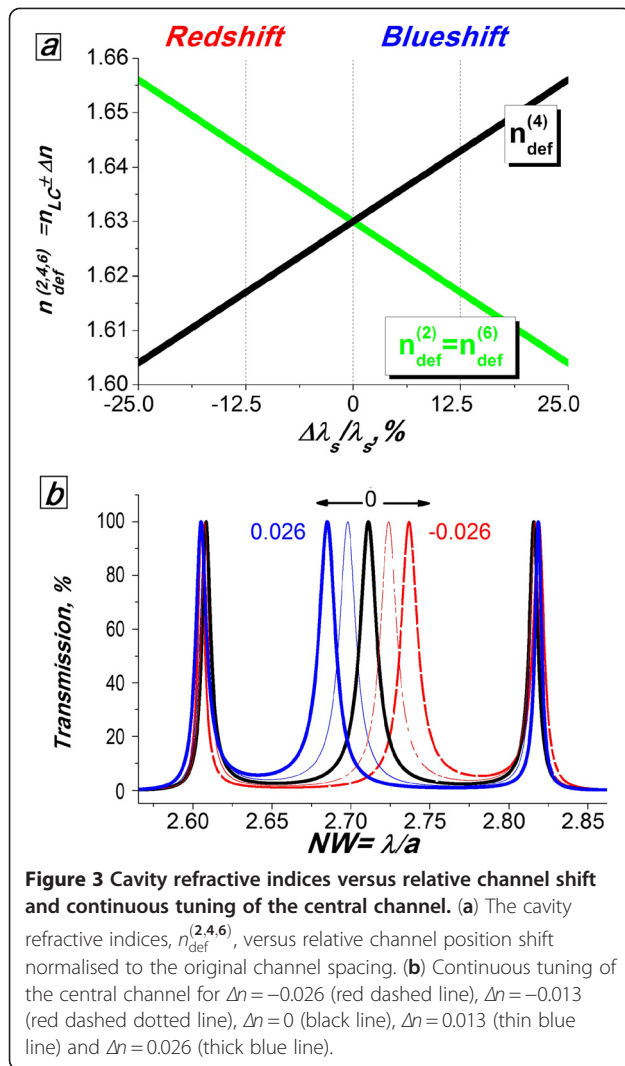
The opposite manipulation of the refractive indices, i.e. reducing $n_{def}^{(4)} = n_{LC} - \Delta n$ while increasing $n_{def}^{(2)} = n_{def}^{(6)} = n_{LC} + \Delta n$, results in an individual red shift of the

central channel (Figure 3b, red dashed dotted and dashed lines). Note that the maximum intensity of $T=100\%$ and the initial bandwidths are unaffected for all switching positions of the triple-channel system.

We now consider the effect of varying the refractive index of the central cavity only in $n_{def}^{(2)} = n_{def}^{(6)} = n_{LC} = 1.63$. The refractive indices of the edge cavities are

Table 2 Deviation of the Si wall thicknesses and channel characteristics for the fabricated triple-cavity PhC

m	$d_{Si} + d_{air}$ (nm)	$d_{Si} \pm \delta d_{Si}$ (nm)	$\pm \Delta \lambda_{c1}$ (nm)	$\pm \Delta \lambda_{c2}$ (nm)	$\pm \Delta \lambda_{c3}$ (nm)	$\lambda_s \pm \Delta \lambda_{s12}$ (nm)	$\lambda_s \pm \Delta \lambda_{s23}$ (nm)
1	1,400	325 ± 35 ($\pm 10.8\%$)	-22	-46.8	-18.5	$153.3 - 24.3$ $153.3 + 27.7$	
2	900	360 ± 20 ($\pm 5.6\%$)	+12.5	+7.7	+12.5	$43 - 6$ $43 + 6$	
3	900	486 ± 20 ($\pm 4\%$)	+4	+5.6	+5.3	$20 - 1$ $20 + 2$	



considered to be fixed at the initial value, $n_{\text{def}}^{(2)} = n_{\text{def}}^{(6)} = n_{\text{LC}} = 1.63$ (Figure 4a). In this case, the central cavity plays the role of a variable intermediate mirror between two strongly coupled edge cavities. The decrease by Δn of the overall optical thickness of the system $n_{\text{def}}^{(2,4,6)} d_{\text{air}} = \lambda_m/2$ results in a blue shift of the edge channels, while the central channel retains its wavelength position. This is clearly demonstrated in Figure 4b for $\Delta n = 0, 0.02, 0.052$ and 0.11 for the structure under consideration. The increase of the channel spacing, $\lambda_s + \Delta\lambda_s$, results in a decrease of the channel spacing between the central channel and the right edge channel, $\lambda_{s2,3} = \lambda_s - \Delta\lambda_s$, lowering the out-of-band reflection between them.

As in the previous model, the overall increase in the refractive index, Δn up to 0.052 , for the example considered, leads to a linear change in the channel spacings of up to 25% or $\lambda_{s12}/\lambda_{s23} = 1.5$ (Figure 4a, b). Although the out-of-band reflection between the central and right

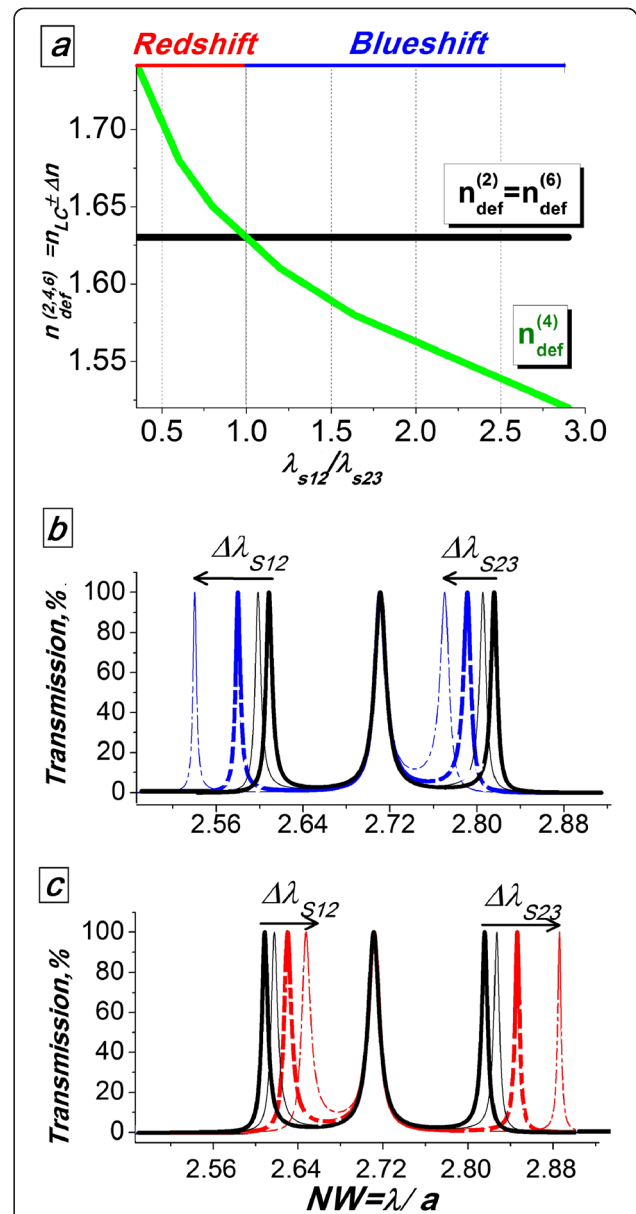


Figure 4 The cavity refractive indices versus relative channel spacings and continuous tuning of the edge channels. (a) The cavity refractive indices $n_{\text{def}}^{(2,4,6)}$ versus the ratio of the channel spacings, $\lambda_{s12}/\lambda_{s23}$. (b) Continuous blue shift of the edge channels with a linear decrease in the central cavity refractive index, $n_{\text{def}}^{(4)}$, by $\Delta n = 0.02$ (thin black line), $\Delta n = 0.052$ (dashed blue line) and $\Delta n = 0.11$ (dashed dotted blue line). The triple transmission channels, for $\Delta n = 0$, are also demonstrated (thick black line). (c) Continuous red shift of the edge transmission channels with a linear increase in the central cavity refractive index, $n_{\text{def}}^{(4)}$, by $\Delta n = 0.02$ (thin black line), $\Delta n = 0.052$ (red dashed line) and $\Delta n = 0.11$ (red dashed dotted line).

edge channel is decreased, it still reaches 95% . Further increases in Δn up to the limiting case of $\Delta n = 0.11$, will result in a rapidly growing difference between channel spacings, $\lambda_{s12}/\lambda_{s23}$ of up to 2.7 with a decrease of the

out-of-band reflection between the central and left-edge channel to 90% (Figure 4b, blue dashed dotted line).

For significantly higher values of $\Delta n \gg 0.11$ than those considered in this paper, the central cavity acts as a single cavity, independent of the edge cavities. The left-edge channel will be shifted out of the SB, and the right edge channel will be merged with the central channel, thus changing the resonator mode from triple mode to single mode. Obviously, the opposite manipulation of the refractive indices, i.e. increasing the $n_{\text{def}}^{(4)} =$

$n_{\text{LC}} + \Delta n$ and fixed $n_{\text{def}}^{(2)} = n_{\text{def}}^{(6)} = n_{\text{LC}}$, results in the individual red shift of the edge channels with the same $\Delta \lambda_s$ value (Figure 4c). Again, as for the central tuning combination, the maximum intensity of $T = 100\%$ is not affected for all switching positions of the triple-channel system.

The tuning approach demonstrated here can be applied to the real devices (Table 2) as previously considered, allowing their actual characteristics to approach those in the original design (Table 1). In Figure 5, this is

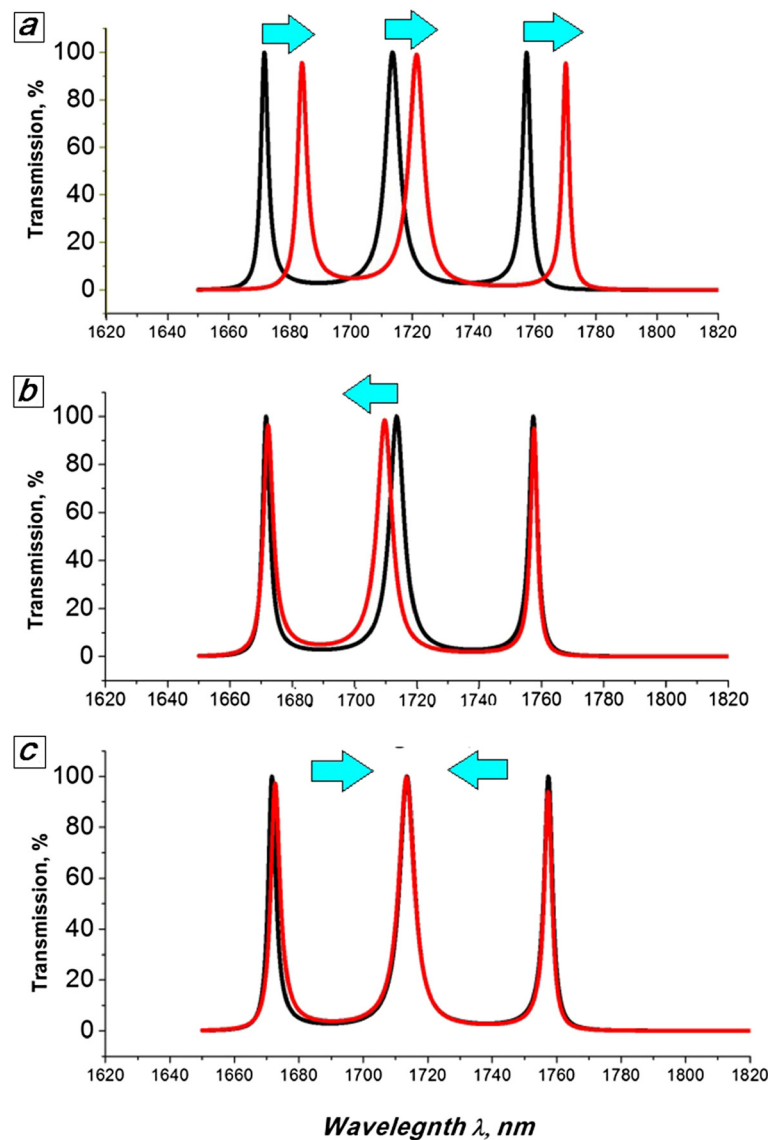


Figure 5 Precise adjustment of the channel wavelength positions of the fabricated device to the originally designed. Transmission spectra of the originally designed triple-defect device operating within the second SB ($m=2$, Table 1) (black line) and of the fabricated device with structural deviations of $\pm \delta d_{\text{Si}} = 20 \text{ nm} = 5.6\%$ ($m=2$, Table 2) (red line). (a) The refractive index of all cavities $n_{\text{def}}^{(2,4,6)} = 1.63$. (b) Precise adjustment of the edge channel wavelength positions of the fabricated device to match those in the original design by decreasing the refractive index to $n_{\text{def}}^{(2,4,6)} = 1.60$. (c) Final adjustment of the central channel with $n_{\text{def}}^{(4)} - \Delta n = 1.60 - 0.01$ and $n_{\text{def}}^{(6)} - \Delta n = 1.60 - 0.01$.

demonstrated for a sample fabricated structure with $m = 2$ (Figure 2a). First, we reduce the refractive index of all cavities, $n_{\text{def}}^{(2,4,6)} = n_{\text{LC}} - \Delta n$, in order to blue shift all three channels. The edge channels are precisely adjusted to the ideal positions when $n_{\text{def}}^{(2,4,6)} = 1.63 - 0.03 = 1.60$ (Figure 5b, red line). Now, we fine tune the central channel by increasing the refractive index of the edge cavities $n_{\text{def}}^{(2,6)} = 1.61 + \Delta n = 1.6 + 0.01 = 1.61$ and reducing the refractive index of the central cavity $n_{\text{def}}^{(4)} = 1.59$ (Figure 5c). The system is now operating at the nominal values in the original design.

Conclusion

To summarise, an approach based on the individual tunability of multi-channel filters has been proposed for the compensation of optical parameter deviations caused by structural fluctuations. Electro-optical tuning of individual central (or edge) channels was demonstrated by up to 25% of the channel spacings, which is sufficient for the optimization of devices with fabrication tolerances of up to 20%. The approach suggested here can be utilised for the optimization of multi-channel silicon devices over a wide infrared range.

Abbreviations

LC: liquid crystal; PhC: photonic crystal; SB: stop band; SEM: scanning electron microscopy; TMM: transfer matrix method.

Competing interests

The authors declare that they have no competing interests.

Authors' contributions

AB is a principle investigator of the project and carried out the simulations, modelling and fabrication of the devices under supervision of TS-P. AB and TS-P designed the manuscript layout. VA-T, KB and TS-P participated in the drafting of the manuscript and helped with the analyses and interpretation of the data. All authors read and approved the final manuscript.

Authors' information

AB is a final year PhD student doing research under supervision of TS-P, professor and director of Microelectronics Technology Group in Trinity College Dublin, Ireland. VA-T is a senior researcher at Ioffe Physical Technical Institute, Russia, and KB is a lecturer at Dublin Institute of Technology, Ireland.

Acknowledgments

This work has been supported by the ICGEE Programme (Ireland) and NAP-368 (Science Foundation Ireland). AB wishes to express the appreciation to Alan Blake (Tyndall Institute Ireland) for the useful discussions.

Author details

¹Department of Electronic and Electrical Engineering, Trinity College Dublin, College Green, Dublin 2, Ireland. ²Ioffe Physical Technical Institute, Polytechnicheskaya 26, St. Petersburg 194021, Russia. ³Department of Electronic and Communications Engineering, Dublin Institute of Technology, Kevin St, Dublin 8, Ireland.

Received: 2 May 2012 Accepted: 5 June 2012
Published: 12 July 2012

References

1. Reed GT: *Silicon Photonics: The State of the Art*. West Sussex: Wiley; 2008.

- Wehrspohn RB, Kitzerow HS, Busch K: *Nanophotonic Materials: Photonic Crystals, Plasmonics, and Metamaterials*. Wiley-VCH: Weinheim; 2008.
- Pavesi L: *Lockwood DJ: Silicon Photonics*. Heidelberg: Springer; 2004.
- Postnikov S, Hector S, Garza C, Peters R, Ivin V: **Critical dimension control in optical lithography**. *Microelectron Eng* 2003, **69**:452–458.
- Baldycheva A, Tolmachev VA, Perova TS: **Fine tunable multi-cavity Si photonic crystal filter**. In *Proceedings of SPIE 2012, 8431, April 16 2012*. Edited by Laurent V, Seppo KH, Pavesi L, Pelli S. Brussels: SPIE Digital Library; 2012:84310H–84310H-13.
- Ghulinyan M, Oton CJ, Gaburro Z, Bettotti P, Pavesi L: **Porous silicon free-standing coupled microcavities**. *Appl Phys Lett* 2003, **82**:1550–1552.
- Mancinelli M, Guider R, Bettotti P, Masi M, Vanacharla MR, Pavesi L: **Coupled-resonator-induced-transparency concept for wavelength routing applications**. *Opt Express* 2011, **19**:12227–12240.
- Atabaki AH, Momeni B, Eftekhari AA, Hosseini ES, Yegnanarayanan S, Adibi A: **Tuning of resonance-spacing in a traveling-wave resonator device**. *Opt Express* 2010, **18**:9447–9455.
- Monat C, Domachuk P, Eggleton BJ: **Integrated optofluidics: a new river of light**. *Nat Photon* 2007, **1**:106–114.
- Alboon SA, Lindquist RG: **Flat top liquid crystal tunable filter using coupled Fabry-Perot cavities**. *Opt Express* 2008, **16**:231–236.
- Weiss S, Ouyang H, Zhang J, Fauchet P: **Electrical and thermal modulation of silicon photonic bandgap microcavities containing liquid crystals**. *Opt Express* 2005, **13**:1090–1097.
- Tolmachev VA, Melnikov VA, Baldycheva AV, Perova TS, Fedulova GI: **Design, fabrication, and optical characterization of Fabry-Prot tunable resonator based on microstructured Si and liquid crystal**. In *Proceedings of SPIE 2010, April 12 2010*. Edited by Miguez HR, Romanov SG, Andreani LC, Seassal C. Brussels, Belgium: SPIE Digital Library; 2010:771320–771312.
- Pucker G, Mezzetti A, Crivellari M, Bellutti P, Lui A, Daldosso N, Pavesi L: **Silicon-based near-infrared tunable filters filled with positive or negative dielectric anisotropic liquid crystals**. *J Appl Phys* 2004, **95**:767–769.
- Cos J, Ferré-Borrull J, Pallarès J, Marsal LF: **Double-cavity Fabry-Pérot tunable equalizer based on 1D photonic crystals**. *Int J Numerical Model: Electron Netw, Devices and Fields* 2010, **23**:400–410.
- Tolmachev VA, Perova TS, Baldycheva AV: **Transformation of one-dimensional silicon photonic crystal into Fabry-Perot resonator**. In *Proceedings of SPIE 2011, 7943 January 22 2011*. Edited by Kubby JA, Reed GT. San Francisco: SPIE Digital Library; 2011:79430E–79410.
- Gaponenko SV: *Introduction to Nanophotonics*. Cambridge: Cambridge University Press; 2010.
- Pavesi L, Gaponenko SV, Negro LD: *Towards the First Silicon Laser*. Dordrecht: Kluwer Academic Publishers; 2003.
- Wang Z, Peng RW, Qiu F, Huang XQ, Wang M, Hu A, Jiang SS, Feng D: **Selectable-frequency and tunable-Q perfect transmissions of electromagnetic waves in dielectric heterostructures**. *Appl Phys Lett* 2004, **84**:3969–3971.
- Mudachathi R, Nair P: **Low-voltage widely tunable photonic crystal channel drop filter in SOI wafer**. *Microelectromechanical Syst, J* 2012, **21**:190–197.
- Tolmachev VA, Melnikov VA, Baldycheva AV, Berwick K, Perova TS: **Electrically tunable Fabry-Perot resonator based on microstructured Si containing liquid crystal**. *Prog In Electromagnetics Res* 2012, **122**:293–309.
- Azzam RMA, Bashara NM: *Ellipsometry and polarized light*. Elsevier Science Publisher: North-Holland; 1987.
- Joannopoulos JD: *Photonic Crystals: Molding The Flow Of Light*. Princeton University Press: Princeton; 2008.
- Pavesi L, Panzarini G, Andreani LC: **All-porous silicon-coupled microcavities: Experiment versus theory**. *Phys Rev B* 1998, **58**:15794–15800.
- Marcuse D: **Coupled mode theory of optical resonant cavities**. *Quantum Electron, IEEE J* 1985, **21**:1819–1826.
- Stanley RP, Houdre R, Oesterle U, Illegems M, Weisbuch C: **Coupled semiconductor microcavities**. *Appl Phys Lett* 1994, **65**:2093–2095.

doi:10.1186/1556-276X-7-387

Cite this article as: Baldycheva et al.: Multi-channel Si-liquid crystal filter with fine tuning capability of individual channels for compensation of fabrication tolerances. *Nanoscale Research Letters* 2012 **7**:387.